Nuclear magnetic resonance relaxation enhancements produced by paramagnetic solutes: Effects of rhombicity in the zero field splitting tensor with the $S=2$ spin system as an example

Jean-Marc Bovet and Robert R. Sharp
Department of Chemistry, The University of Michigan, Ann Arbor, Michigan 48109

(Received 21 December 1992; accepted 23 March 1993)

Effects due to the nonuniaxial part of the zero field splitting (ZFS) tensor on NMR relaxation enhancements produced by paramagnetic species in solution (the NMR PRE) has been studied theoretically and experimentally in the ZFS limit, i.e., in the limit where the ZFS energy is large compared to the Zeeman energy. In the ZFS limit, the precessional motion of the electron spin is quantized with respect to molecule-fixed coordinate axes. The uniaxial part of the ZFS tensor induces precessional motion in the transverse (x,y) components of the electron spin vector S, and x,y anisotropy in the ZFS tensor (i.e., a nonzero ZFS parameter E) induces precessional motion in the z component of S. The NMR-PRE phenomenon is particularly sensitive to the motion of S_z and hence also to ZFS anisotropy in the xy plane. Mathematical expressions have been derived which describe the motion of the spin vector evolving under the influence of a general rhombic ZFS Hamiltonian and the influence of this motion on the NMR PRE in the ZFS limit. It is shown that oscillations in S_z occur at the transition frequencies of the S spin system; the frequencies and amplitudes of the precessional components of S_z can be calculated by diagonalizing the general ZFS Hamiltonian. These motions and their consequences with respect to the behavior of the NMR PRE are described in detail for the $S=2$ spin system. A parametrization of NMR-PRE data is proposed which gives a clear criterion for the conditions under which rhombic parts of the ZFS tensor significantly affect the relaxation enhancements produced by an $S=2$ spin system. This criterion is of considerable practical importance for the analysis of NMR-PRE data, since it defines conditions under which data may be analyzed without the need for independent experimental information concerning the magnitude of the ZFS tensor.

I. INTRODUCTION

Dissolved paramagnetic metal ions in solution frequently produce profound enhancements of the nuclear spin relaxation rates of solvent nuclei as well as of ligand species that are coordinated to the metal. This phenomenon is termed the NMR paramagnetic relaxation enhancement or NMR PRE. Physically, the NMR PRE arises from time-dependent dipolar and scalar magnetic hyperfine couplings between the nuclear and electron spins. The time dependence of these couplings is very sensitive to the motion of the electron spin, which has both precessional and stochastic components (the latter associated with electron spin relaxation).

Two physical limits concerning the motion of the electron spin can be distinguished. First is the Zeeman limit, in which the Zeeman energy is large compared to the zero field splitting (ZFS) energy. In this situation, the precessional motion of the electron spin is quantized with respect to the external magnetic field. The stochastic time dependence associated with spin relaxation is superimposed on this precessional motion. In the ZFS limit, the ZFS energy is large compared to the Zeeman energy. In this latter situation, the electron spin precesses about molecule-fixed coordinate axes rather than about the external field axis.

Since the NMR PRE depends critically on the motion of the electron spin, its properties differ substantially in these two limits. The traditional theory of the NMR PRE is appropriate to the Zeeman limit and was developed more than three decades ago by Solomon,[1] Bloembergen,[2,3] and Morgan[3] (SBM theory). Very widely used in practical studies, SBM theory is a limiting theory which is often physically inappropriate for large ZFS ions, as well as in studies where the ZFS is smaller but the magnetic field strength low (as typically occurs in magnetic resonance imaging). For this reason, theory has more recently been developed in this[4–9] and other[10–23] laboratories which incorporates the effects of both ZFS and Zeeman interactions. Our approach, which is similar to that of Fukui, Miura, and Matsuda[23] involves a density matrix formulation in which the motion of the electron spin operators is described in the natural coordinate system (molecule fixed or laboratory fixed) of the electron spin Hamiltonian. Using this approach, simple analytical expressions have been derived[4,5] which parallel the form of the corresponding expressions of SBM theory but are appropriate for the uniaxial ZFS limit. Theory that bridges the ZFS- and Zeeman-limit regimes has also been derived[6,23] and has been implemented in the program PARELAX.[6] ZFS interactions give rise to striking qualitative phenomena in the NMR PRE which have no analog in the Zeeman limit. Qualitative aspects of these phenomena have been described systematically for spin systems with $S=1$ (Ref. 7) and $S>1$.[8]

In recent work[9,23] it has been shown that the presence

 0021-9606/93/99(1)/18/9/$6.00

of (x,y) anisotropy in the ZFS tensor, i.e., a nonzero E parameter, can in the ZFS limit have very profound effects on the NMR PRE which differ qualitatively in character from those produced by the uniaxial part of the ZFS tensor. This situation results from the fact that the E term of the ZFS Hamiltonian, unlike the uniaxial term (that proportional to the ZFS parameter D), induces precessional motion in the z component of the electron spin. The present study concerns the general (nonuniaxial) ZFS limit, for which new closed form expressions for the NMR PRE are derived for the magnetic-dipole–magnetic-dipole and scalar relaxation mechanisms. These expressions are cast in a mathematical form which clearly relates the physical properties of the precessional motion of the electron spin to the behavior of the NMR PRE. The specific behavior of the $S=2$ spin system is elaborated in some detail. The theory of the effects of ZFS rhombicity that is presented below differs from our earlier theory[9] in that the latter was suitable for numerical calculations but, unlike the present treatment, was not cast in a form which provided a transparent qualitative picture of the effect of the ZFS E term on the motion of the electron spin vector and on the NMR PRE.

The present theory has been applied to NMR-PRE data for the methyl proton resonance of *tris*-[acetylacetonato]Mn(III) ($Mn[acac]_3$), which contains high-spin Mn(III), a d^4 ion with $S=2$. At magnetic field strengths below about 2 T, the $Mn[acac]_3$ spin system is well described by the ZFS limit. Its associated NMR PRE has previously been studied in detail using theory[5,6,24,25] which accounts for the Zeeman interaction plus the uniaxial part of the ZFS tensor. The analysis of these data is reconsidered below using the theory developed here and in Ref. 9 in order to better understand the role of ZFS rhombicity.

II. THE ELECTRON SPIN HAMILTONIAN

The precessional motion of the electron spin is induced by the static part of the electron spin Hamiltonian, $H_S = \hbar\mathcal{H}_S$, where

$$\mathcal{H}_S = \mathcal{H}_Z + \mathcal{H}_{ZFS} + \mathcal{H}_{hf}. \tag{1}$$

The terms on the right-hand side of Eq. (1) are the Zeeman, the quadratic zero field splitting, and the electron-nuclear hyperfine contributions to $\mathcal{H}_S$, given by

$$\mathcal{H}_Z = \mathbf{g}\beta B_0 S_z, \tag{2a}$$

$$\mathcal{H}_{ZFS} = \mathcal{H}_{ZFS}^{(D)} + \mathcal{H}_{ZFS}^{(E)}$$

$$= \omega_D(\hat{S}_z^2 - 3^{-1}S(S+1)) + \omega_E(\hat{S}_x^2 - \hat{S}_y^2) \tag{2b}$$

$$= (\tfrac{2}{3})^{1/2}\omega_D\hat{S}_0^{(2)} + \omega_E(\hat{S}_{+2}^{(2)} + \hat{S}_{-2}^{(2)}), \tag{2c}$$

$$\mathcal{H}_{hf} = \mathbf{I}\cdot\mathbf{A}\cdot\mathbf{S}. \tag{2d}$$

The spin variables in Eqs. (2a)–(2c) are expressed in different coordinate systems. We use the convention that spin variables and functions of spin variables that are written without a superscripting caret (e.g., S_z) are expressed in a laboratory coordinate frame in which the z axis is parallel to the external magnetic field. Spin variables and functions written with a superscripting caret ($\hat{S}_z$) are expressed in the molecule-fixed coordinate frame which diagonalizes the ZFS tensor. $\hat{S}_0^{(2)}$ and $\hat{S}_{\pm 2}^{(2)}$ are spherical tensor forms of the spin operators, the definitions and matrix representations of which are given in the Appendix. $\mathcal{H}_{ZFS}$ is nonzero for electron spins $S > 1/2$ in nonspherical site symmetry; this situation will be assumed in the following discussion. $\mathbf{g}$ is the electron spin $\mathbf{g}$ value, β is the Bohr magneton, B_0 is the laboratory magnetic induction, ω_D and ω_E are the ZFS parameters D and E (in cm^{-1}) expressed in rad s^{-1} (e.g., $\omega_D = 2\pi c D$), and $\mathbf{A}$ is the electron-nuclear hyperfine coupling tensor. Equations (2b) and (2c) neglect quartic terms in $\mathcal{H}_{ZFS}$, which are nonzero for $S \geqslant 2$ although normally small. The precessional motion of $\mathbf{S}$ arises from the static parts of $\mathcal{H}_S$, while electron and nuclear spin relaxation phenomena originate in the time dependent parts of $\mathcal{H}_S$. Stochastic fluctuation of $\mathcal{H}_{ZFS}$ provides (for $S > 1/2$) the principal mechanism of electron spin relaxation, and stochastic fluctuations in $\mathcal{H}_{hf}$ give rise to the NMR PRE. $\mathcal{H}_{hf}$ is composed of additive terms due to electron-nuclear magnetic dipole and scalar (Fermi contact) interactions, which produce additive dipolar and scalar contributions to the paramagnetic part, $R_{1m}(=1/T_{1m})$, of the nuclear spin relaxation rate.

Quantization axes of the precessional motion of the electron spin are determined fundamentally by the relative magnitudes of $\mathcal{H}_Z$ and $\mathcal{H}_{ZFS}$. The Zeeman limit corresponds to $\mathcal{H}_Z \gg \mathcal{H}_{ZFS}$, the general (anisotropic) ZFS limit corresponds to $\mathcal{H}_{ZFS} \gg \mathcal{H}_Z$, and the uniaxial ZFS limit corresponds to ($\mathcal{H}_{ZFS}^{(D)} \gg \mathcal{H}_Z, \mathcal{H}_{ZFS}^{(E)}$). The behavior of the NMR PRE differs profoundly in these three limits in ways which have been described in considerable detail previously.[7–9,23]

III. MOTION OF THE ELECTRON SPIN AND ITS EFFECT ON THE NMR PRE

Physically, the NMR PRE depends on the Fourier components of the electron-nuclear magnetic hyperfine interaction (which is composed of dipolar and/or scalar couplings) at the transition frequencies of the coupled I-S spin system. For this reason, R_{1m} depends critically on the motion of the S spin. The objective of the present section is to describe the effect of ZFS rhombicity (i.e., the E term) on the motion $\mathbf{S}$ and to show, physically and mathematically, how this motion affects the nuclear spin relaxation rate.

For this purpose, the theoretical expressions for the paramagnetic relaxation enhancement will be expressed in a form which isolates the dependence of R_{1m} on $\mathbf{S}(t)$. The motion of $\mathbf{S}$ appears in the NMR relaxation theory in the form of the time correlation functions $G_z(t)$ and $G_\pm(t)$ of the longitudinal and transverse components of the electron spin,

$$G_z(t) \equiv \mathrm{Tr}\{\rho(t)S_z(t)S_z(0)\}, \tag{3}$$

$$G_\pm(t) \equiv \mathrm{Tr}\{\rho(t)S_\pm(t)S_\mp(0)\}, \tag{4}$$

where ρ is the density matrix for the S spin manifold. Normally the electron spin system remains at thermal equilibrium during NMR experiments. Assuming that this is true and that the S spin system is in the high temperature limit implies that $\rho(t)=\rho_0=(2S+1)^{-1}\,\mathbf{1}$, where ρ_0 is the density matrix of the S spin manifold at thermal equilibrium and high temperature, and $\mathbf{1}$ is the unit matrix. The motions of $S_z(t)$ and $S_\pm(t)$ contribute additively to R_{1m}. For the uniaxial ZFS limit, the electron spin variables are most conveniently expressed in the molecular coordinate frame. Theory[6,9] gives

$$R_{1m}=\hat{R}_{1m}^{(z)}+2^{-1}(\hat{R}_{1m}^{(+)}+\hat{R}_{1m}^{(-)}), \tag{5}$$

where $\hat{R}_{1m}^{(z)}$ and $\hat{R}_{1m}^{(\pm)}$ are Fourier integrals of the functions $\hat{G}_z(t)$ and $\hat{G}_\pm(t)$:

$$\hat{R}_{1m}^{(z)}=b_z(r,\Theta)\int_0^\infty \hat{G}_z(t)\exp[(i\omega_I-\tau_R^{-1})t]dt, \tag{6a}$$

$$\hat{R}_{1m}^{(\pm)}=b_\pm(r,\Theta)\int_0^\infty \hat{G}_\pm(t)\exp[(i\omega_I-\tau_R^{-1})t]dt. \tag{6b}$$

Likewise, Zeeman-limit theory can be cast in a similar form, where R_{1m} is written as a sum of terms $R_{1m}^{(z)}$ and $R_{1m}^{(\pm)}$. In both limiting theories, $\hat{R}_{1m}^{(z)}$ and $R_{1m}^{(z)}$ correspond to the "low frequency" part of R_{1m} [that proportional to the spectral density function $j(\omega_I)$], and $\hat{R}_{1m}^{(\pm)}$ and $R_{1m}^{(\pm)}$ correspond to the "high frequency" parts of R_{1m} [those proportional to $j(\omega_S\pm\omega_I)$ in Zeeman-limit theory or to $j(\omega_\mu\pm\omega_I)$ in the uniaxial ZFS-limit theory]. ω_I and ω_S are the nuclear and electron Larmor precession frequencies, and the ω_μ are the one-quantum transition frequencies of the S-spin system in the ZFS limit. The functions $b_z(r,\Theta)$ and $b_\pm(r,\Theta)$ depend on the strength and geometry of the magnetic dipole coupling interaction, but not on the motion of $\mathbf{S}(t)$. In uniaxial ZFS-limit theory of dipole–dipole relaxation,

$$b_z(r,\Theta)=\frac{4}{3}\gamma_I^2\mathbf{g}^2\beta^2\mathbf{r}^{-6}\left(\frac{\mu_0}{4\pi}\right)^2[1+P_2(\cos\Theta)], \tag{7a}$$

$$b_\pm(r,\Theta,\Phi)=b_\pm(r,\Theta)=\frac{4}{3}\gamma_I^2\mathbf{g}^2\beta^2\mathbf{r}^{-6}\left(\frac{\mu_0}{4\pi}\right)^2[1-2^{-1}P_2(\cos\Theta)]. \tag{7b}$$

where γ_I is the nuclear gyromagnetic ratio, μ_0 is the magnetic permeability of free space, r is the I-S interspin distance, $P_2(x)$ is the second-order Legendre polynomial, and Θ and Φ are the polar angles of the I-S vector in the molecule-fixed coordinate frame which diagonalizes the ZFS tensor. In Eqs. (6), $\tau_R=\tau_R^{(1)}$ is a reorientational correlation time for a molecule-fixed first-rank spherical tensor.

The most common physical situation is that $\hat{R}_{1m}^{(z)}\gg\hat{R}_{1m}^{(\pm)}$ in the uniaxial ZFS limit, and likewise that $R_{1m}^{(z)}\gg R_{1m}^{(\pm)}$ in the Zeeman limit. In other words, it is the time dependence of the z component of $\mathbf{S}$ which gives rise to the major part of the T_1 NMR PRE. This reflects the fact that the transverse components of $\mathbf{S}$ undergo rapid precessional motions which, when $\omega_\mu\tau_c>1$, where τ_c is the correlation time of the magnetic dipole interaction, reduce the integral of Eq. (6b) to a small value. In contrast, $\hat{S}_z$ and $\hat{G}_z$ do not precess in the uniaxial ZFS limit (nor do S_z and G_z in the Zeeman limit), their only time dependence being stochastic motion that is associated with electron spin relaxation. As a result, $\hat{G}_z(t)$ [or $G_z(t)$] typically persists for much longer times than does $\hat{G}_\pm(t)$ [or $G_\pm(t)$]. When this is true, $R_{1m}\approx\hat{R}_{1m}^{(z)}\gg\hat{R}_{1m}^{(\pm)}$.

When ZFS rhombicity is significant in the ZFS limit, this picture changes profoundly since then $\hat{S}_z$, like $\hat{S}_\pm$, precesses. The precessional motion of $\hat{S}_z$ is described by oscillatory time dependence in $\hat{G}_z(t)$, and when significant precession occurs on the time scale of τ_c, this motion acts to depress $\hat{R}_{1m}^{(z)}$. In the following we develop an explicit algebraic expression for $\hat{G}_z(t)$ in the ZFS limit when the ZFS tensor contains both uniaxial (D) and rhombic (E) terms. We also have the more general objective of developing a clear physical picture of the motion of $\mathbf{S}$ under $\mathscr{H}_{\mathrm{ZFS}}$ and of the consequences of this motion on the behavior of the NMR PRE.

The trace in Eq. (3) can be evaluated by writing $\hat{S}_z(t)$ in the Heisenberg representation,

$$\hat{S}_z(t)=\exp(-i\mathscr{H}_{\mathrm{ZFS}}t)\hat{S}_z(0)\exp(i\mathscr{H}_{\mathrm{ZFS}}t), \tag{8}$$

and evaluating the sum in the eigensystem $\{|\mu\rangle,|\nu\rangle;\epsilon_\mu,\epsilon_\nu\}$ of $\mathscr{H}_{\mathrm{ZFS}}$. We assume that the S spin system remains at thermal equilibrium in the high temperature limit so that its wave function is

$$|\psi_S\rangle=(2S+1)^{-1/2}\sum_\mu|\mu\rangle. \tag{9}$$

Using Eqs. (3), (8), and (9) and the closure relation gives

$$\hat{G}_z(t)=(2S+1)^{-1}\exp(-t/\tau_S)\sum_{\mu,\nu}\exp[i(-\epsilon_\mu+\epsilon_\nu)t]\times\langle\mu|\hat{S}_z(0)|\nu\rangle\langle\nu|\hat{S}_z(0)|\mu\rangle. \tag{10}$$

In Eq. (10), electron spin relaxation, which results from stochastic time dependence in $\mathscr{H}_S(t)$, has been described by a single exponential factor, $\exp(-t/\tau_S)$.

In evaluating $\hat{G}_z(t)$, it should be noted that $\hat{S}_z$ is diagonal in the eigenbasis $|m\rangle$ of $\mathscr{H}_{\mathrm{ZFS}}^{(D)}$ but not in the eigenbasis $|\mu\rangle$ of $\mathscr{H}_{\mathrm{ZFS}}=\mathscr{H}_{\mathrm{ZFS}}^{(D)}+\mathscr{H}_{\mathrm{ZFS}}^{(E)}$. To evaluate the matrix elements $\langle\mu|\hat{S}_z|\nu\rangle$, the eigenvectors $|\mu\rangle$ of $\mathscr{H}_{\mathrm{ZFS}}$ are expanded in the eigenbasis $|m\rangle$ of $\mathscr{H}_{\mathrm{ZFS}}^{(D)}$,

$$|\mu\rangle=\sum_m c_{\mu,m}|m\rangle. \tag{11}$$

The fact that $[\hat{S}_z,\mathscr{H}_{\mathrm{ZFS}}^{(D)}]=0$ implies that $\langle n|\hat{S}_z|m\rangle=m\delta_{mn}$, giving

$$\hat{G}_z(t)=(2S+1)^{-1}\exp(-t/\tau_S)\sum_{\mu,\nu}\exp[i(-\epsilon_\mu+\epsilon_\nu)t]\times\sum_{m,m'}c_{\mu,m}^*c_{\nu,m}c_{\nu,m'}^*c_{\mu,m'}mm'. \tag{12}$$

Inspection of Eq. (12) shows that there is no contribution to $\hat{G}_z(t)$ from terms with $m=0$ or $m'=0$, and it can also be

shown that terms for which $\mu=\nu$ vanish. The form of $\hat{G}_z(t)$ can be simplified by defining the coefficients

$$g_\lambda \equiv g_{\mu,\nu}=g_{\nu,\mu}=\sum_{m,m'} c^*_{\mu,m}c_{\nu,m}c^*_{\nu,m'}c_{\mu,m'}mm', \tag{13}$$

and the transition frequencies, $\omega_\lambda=|\epsilon_\nu-\epsilon_\mu|$ $(\nu>\mu)$. Equation (12) can then be written

$$\hat{G}_z(t)=(2S+1)^{-1}\exp(-t/\tau_S)\sum_\lambda g_\lambda[\exp(i\omega_\lambda t)+\exp(-i\omega_\lambda t)]$$

$$=2(2S+1)^{-1}\exp(-t/\tau_S)\sum_\lambda g_\lambda\cos(\omega_\lambda t), \tag{14}$$

where the sum in Eq. (14) is over transitions λ for which $\nu>\mu$. Hence the motion of $\hat{G}_z(t)$ consists of an exponentially damped sum of oscillatory components, the frequencies of which are the transition frequencies ω_λ of the S spin system.

Inserting Eq. (14) in Eq. (6a) and integrating gives the following form for $\hat{R}^{(z)}_{1m}$:

$$\hat{R}^{(z)}_{1m}=b_z(r,\Theta)(2S+1)^{-1}\sum_\lambda g_\lambda[\,j(\omega_\lambda+\omega_I)+j(\omega_\lambda-\omega_I)\,]. \tag{15}$$

Thus the principal effect of ZFS rhombicity on the NMR PRE is that the low frequency term, $\hat{R}^{(z)}_{1m}$, which is proportional to $j(\omega_I)$ in the uniaxial-ZFS limit, is replaced by a sum of terms proportional to $j(\omega_I\pm\omega_\lambda)$, where ω_λ are transition frequencies of the S spin system. Since ω_λ is nearly always much larger than ω_I, the precessional motions of $\hat{G}_z(t)$ act to depress $\hat{R}^{(z)}_{1m}$, strongly so when $\omega_\lambda\tau_c>1$.

Equation (15) describes the intramolecular magnetic-dipole–dipole relaxation mechanism. The scalar contribution to R_{1m} can likewise be written as a sum of terms due to the longitudinal and transverse components of S,

$$R_{1m,\mathrm{sc}}=\hat{R}^{(z)}_{1m,\mathrm{sc}}+2^{-1}(\hat{R}^{(+)}_{1m,\mathrm{sc}}+\hat{R}^{(-)}_{1m,\mathrm{sc}}). \tag{16}$$

Following the treatment of Ref. 4, the longitudinal term $\hat{R}^{(z)}_{1m,\mathrm{sc}}$ is

$$\hat{R}^{(z)}_{1m,\mathrm{sc}}=3^{-1}A^2\int_0^\infty \hat{G}_z(t)\exp(-t/\tau_R^{(1)}-t/\tau_{\mathrm{con}})\times[\exp(i\omega_I t)+\exp(-i\omega_I t)]\,dt \tag{17}$$

$$=3^{-1}A^2(2S+1)^{-1}\sum_\lambda 2g_\lambda[\,j(\omega_\lambda+\omega_I)+j(\omega_\lambda-\omega_I)\,]. \tag{18}$$

A is the scalar coupling constant in rad s^{-1}. The scalar correlation time τ_{sc} in the ZFS limit is defined by

$$(\tau_{\mathrm{sc}})^{-1}=(\tau_R^{(1)})^{-1}+(\tau_S)^{-1}+(\tau_{\mathrm{con}})^{-1}, \tag{19}$$

where τ_{con} is a correlation time which describes time dependence in the scalar coupling constant A as may arise, for example, due to chemical exchange reactions.

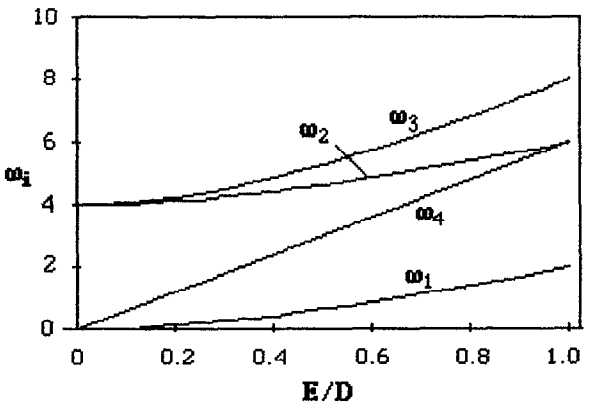

FIG. 1. Transition frequencies (in units of ω_D) of an $S=2$ spin system that is subject to the quadratic uniaxial zero field splitting Hamiltonian of Eq. (2d). The transition frequencies plotted are those associated with nonvanishing amplitudes g_i as defined by Eq. (13).

IV. MOTION OF THE SPIN FOR $S=2$

This result is now elaborated for $S=2$. The amplitudes g_λ and transition frequencies ω_λ can be computed by diagonalizing $\mathscr{H}_{\mathrm{ZFS}}$. For this purpose, $\mathscr{H}_{\mathrm{ZFS}}$ must be expressed in matrix form in the molecular coordinate frame that diagonalizes the ZFS tensor. The appropriate matrix forms of $\hat{S}^{(2)}_0$ and $\hat{S}^{(2)}_{\pm2}$ are given in the Appendix. $\mathscr{H}^{(D)}_{\mathrm{ZFS}}$ is diagonal with eigenbasis $|m\rangle$ in this coordinate frame. The spin operator $\hat{S}^{(2)}_{\pm2}$ in $\mathscr{H}^{(E)}_{\mathrm{ZFS}}$ mixes eigenstates of $\mathscr{H}^{(D)}_{\mathrm{ZFS}}$ for which $\Delta m_S=\pm2$. This is reflected in the form of the transformation matrix defined by Eq. (11), which is

$\|1\rangle$	$\|2\rangle$	$\|3\rangle$	$\|4\rangle$	$\|5\rangle$	
$c_{+2,1}$	0	$c_{+2,3}$	0	$c_{+2,5}$	$\|+2\rangle$
0	$c_{+1,2}$	0	$c_{+1,4}$	0	$\|+1\rangle$
$c_{0,1}$	0	$c_{0,3}$	0	$c_{0,5}$	$\|0\rangle$
0	$c_{-1,2}$	0	$c_{-1,4}$	0	$\|-1\rangle$
$c_{-2,1}$	0	$c_{-2,3}$	0	$c_{-2,5}$	$\|-2\rangle$.

The eigenvectors $|\mu\rangle$ of $\mathscr{H}_{\mathrm{ZFS}}$ occur as two groups, $\{|\mu_1\rangle,|\mu_3\rangle,|\mu_5\rangle\}$ and $\{|\mu_2\rangle,|\mu_4\rangle\}$. The first of these consists of linear combinations of the $\{|+2\rangle,|0\rangle,|-2\rangle\}$ states; the second, linear combinations of the $\{|+1\rangle,|-1\rangle\}$ states. Off-diagonal matrix elements between the two sets vanish (equivalently, only states with $\Delta m=\pm2$ are coupled by $\mathscr{H}^{(E)}_{\mathrm{ZFS}}$). According to Eq. (13) there are four eigenfrequencies of the spin system that have nonvanishing amplitudes g_λ, namely, $\{\omega_1=\epsilon_1-\epsilon_5,\ \omega_2=\epsilon_1-\epsilon_3,\ \omega_3=\epsilon_3-\epsilon_5\}$, which are transition frequencies between eigenstates of the first set, and $\{\omega_4=\epsilon_2-\epsilon_4\}$ between the eigenstates of the second set.

Figures 1 and 2 illustrate the precessional behavior of $\hat{G}_z(t)$. The eigenfrequencies ω_λ (in units of ω_D) and amplitudes g_λ are shown as a function of the E/D ratio. It is clear from the figures that when $E/D\to0$, the only nonvanishing contributions to $\hat{G}_z(t)$ are those with zero frequency, g_1 and g_4. In other words, when $E=0$, $\hat{S}_z(t)$ is static (which also follows from the fact that $[\hat{S}_z,\mathscr{H}^{(D)}_{\mathrm{ZFS}}]=0$). As E/D increases, ω_4, which describes spin motion

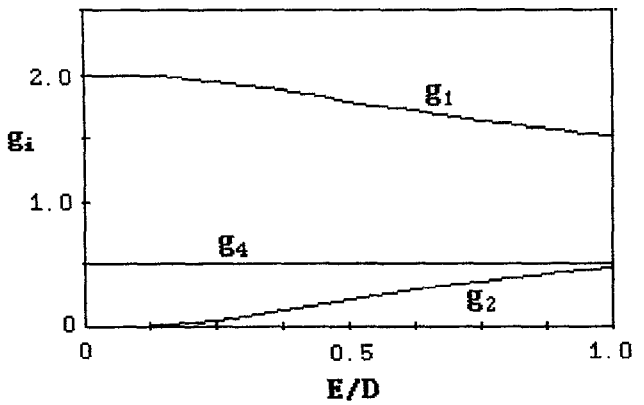

FIG. 2. Amplitudes of the oscillating components of the time correlation function $G_z(t)$ as a function of the ratio of ZFS parameters E/D. The amplitudes are defined in Eq. (13).

in the $\{|+1\rangle,|-1\rangle\}$ states, increases linearly with E/D, while ω_1 increases quadratically and much more slowly. Thus the ω_4 contribution to R_{1m} falls off much more rapidly with increasing E/D than does the contribution due to ω_1. The two eigenfrequencies, ω_1 and ω_4, that contribute to $G_z(0)$ account respectively for 80% and 20% of the total amplitude. Figure 3 shows the dependence of $\hat{R}_{1m}^{(z)}$ on E/D, with the reduced dipolar correlation time $\omega_D\tau_c$ set to 15. $\hat{R}_{1m}^{(z)}$ decreases in a biphasic manner, dropping by 20% in the region where $E/D<0.02$, and the remaining 80% in the vicinity of $E/D\approx 0.15$. Clearly, these two phases result from the precessional motions of $\hat{G}_z(t)$ that are associated with eigenfrequencies ω_4 and ω_1.

Figures 4 and 5 illustrate the time-domain behavior of the spin populations of an $S=2$ spin system under the influence of the general rhombic ZFS Hamiltonian. These plots were computed by direct numerical integration of the density matrix $\rho(t)$, expressed in the eigenbasis of $\mathscr{H}_{\mathrm{ZFS}}^{(D)}$, using the Heisenberg representation of the operator,

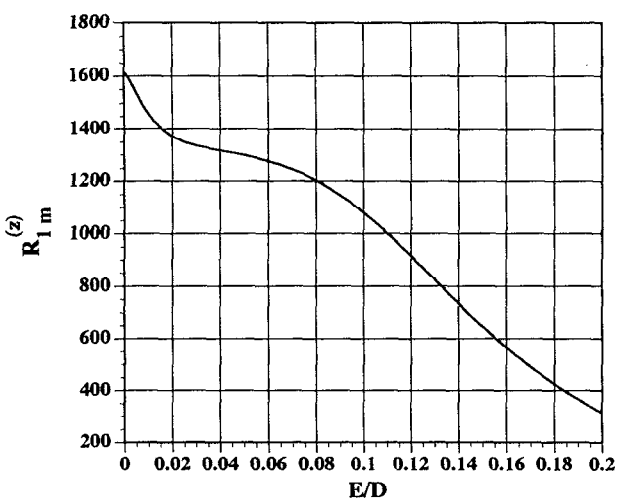

FIG. 3. Dependence of $\hat{R}_{1m}^{(z)}$ [defined by Eq. (6a)] on the ratio of ZFS parameters E/D in the anisotropic ZFS limit.

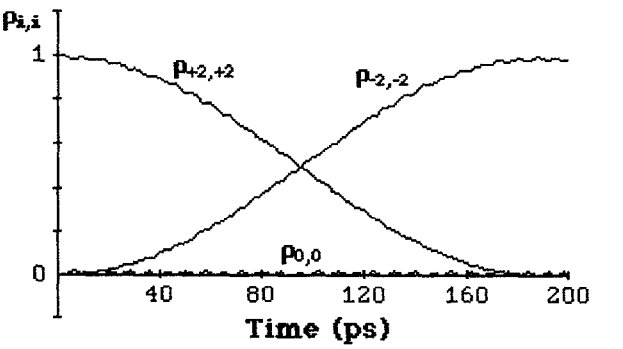

FIG. 4. Time evolution of the diagonal elements of the density matrix $\rho(t)$ of an $S=2$ spin system that precesses under the influence of a static anisotropic ZFS Hamiltonian of the form of Eq. (2d). The spin system was prepared in the $|+2\rangle$ state at $t=0$, so that $\rho_{+2,+2}(0)=1$ at $t=0$ and all other density matrix elements $\rho_{i,j}(0)$ are zero. The elements $\rho_{+1,+1}$ and $\rho_{-1,-1}$ remain zero at all t. The time evolution of $\rho_{ij}(t)$ was calculated by finite numerical integration of the equation of motion of the density operator [Eq. (16)]. The exponential propagator was written using the matrix representation of $\mathscr{H}_{\mathrm{ZFS}}$ that is given in the Appendix, terms up to fifth order in the exponential operator being retained. Finite time steps of 0.2 ps were used in the calculation. The assumed ZFS parameters were $D=3\ \mathrm{cm}^{-1}$, $E/D=0.1$.

$$\rho(t)=\exp(-i\mathscr{H}_{\mathrm{ZFS}}t)\rho(0)\exp(i\mathscr{H}_{\mathrm{ZFS}}t). \tag{20}$$

Figure 4 shows the time evolution of the diagonal matrix elements of $\rho(t)$ when the spin system is initially prepared in the $|+2\rangle$ state at $t=0$, with $D=3\ \mathrm{cm}^{-1}$ and $E/D=0.1$. Under $\mathscr{H}_{\mathrm{ZFS}}$ there is no mixing of the $\{|+2\rangle,|0\rangle,|-2\}$ states with the $\{|+1\rangle$ and $|-1\rangle\}$ states. Thus $\rho_{+1,+1}$ and $\rho_{-1,-1}$ both remain zero at all t. The low frequency (ω_1) oscillation of $\rho(t)$ interchanges the $|+2\rangle$ and $|-2\rangle$ populations. The ω_2 and ω_3 terms are small in amplitude and produce a high frequency admixture of the $|0\rangle$ state with the $|+2\rangle$ and $|-2\rangle$ states. Figure 5 illustrates the behavior of the same spin system prepared at $t=0$ in the $|+1\rangle$ state. In this case, the spin populations oscillate between the $|+1\rangle$ and $|-1\rangle$ states with the single transition frequency ω_4, where $\omega_4 \gg \omega_1$.

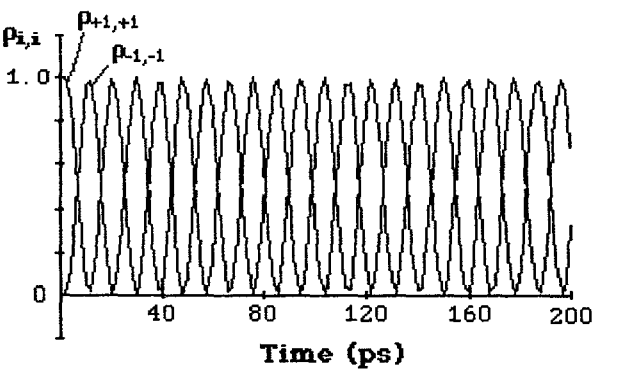

FIG. 5. Time evolution of the diagonal elements of the density matrix $\rho(t)$ of an $S=2$ spin system that precesses under the influence of a static anisotropic ZFS Hamiltonian. All details of the calculation are the same as for Fig. 4, except that the spin system was initially prepared in the $|+1\rangle$ state, so that $\rho_{+1,+1}(0)=1$, and all other $\rho_{i,j}(0)=0$.

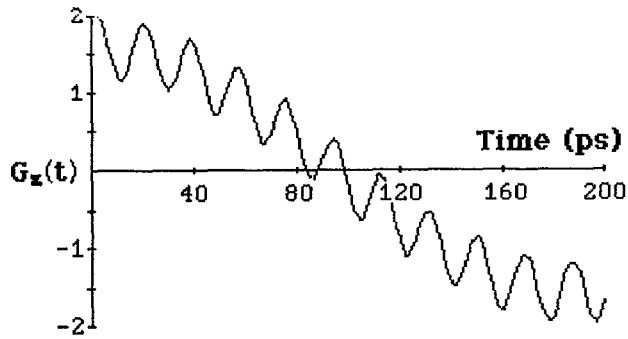

FIG. 6. Evolution of the time correlation function $G_z(t)$ for an $S=2$ spin system which is under the influence of an anisotropic ZFS Hamiltonian $\mathscr{H}_{\rm ZFS}$ at thermal equilibrium. $G_z(t)$ was calculated by direct numerical integration of the exponential form of the spin operator [Eq. (8)]. The calculation was similar to that described in the legend of Fig. 4, except that the spin system was at thermal equilibrium.

Figure 6 shows the time evolution of the time correlation function $\hat{G}_z(t)$, calculated by direct numerical integration of Eqs. (3) and (8) for an ensemble of spins, $S=2$, in thermal equilibrium. The plot clearly shows the two major oscillatory components (ω_1 and ω_4) which contribute to $\hat{G}_z(t)$ at small E/D. The higher (ω_4) and lower (ω_1) frequency terms are responsible for the two phases of the R_{1m} vs E/D plot that were discussed above (see Fig. 3).

V. THE RESONANT PART OF R_{1m}

It has been shown previously that the transverse part of R_{1m} [that due to $\hat{G}_{\pm}(t)$] exhibits resonant behavior in which the term $\hat{R}_{1m}^{(\pm)}$ becomes large at the energy level crossings of the S spin system. Physically, this behavior corresponds to resonance between the precessional motions associated with $\mathscr{H}_{\rm ZFS}^{(D)}$ and $\mathscr{H}_{\rm ZFS}^{(E)}$. For an $S=1$ spin system, $\hat{R}_{1m}^{(\pm)}$ shows a simple resonance at $2\omega_E=\omega_D$, the functional dependence of which has been discussed previously.[9]

The situation for $S=2$ is more complex. The energy level diagram (energy in units of $\hbar\omega_D$ vs E/D) is shown in Fig. 7. There are two level crossings, one of which involves a near degeneracy of the $|\mu_1\rangle$ and $|\mu_5\rangle$ levels over a broad range of E/D ratios centered around $E/D=1$, the other of

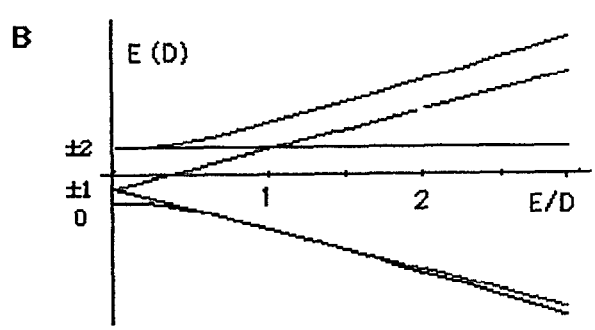

FIG. 7. Energy level diagram of an $S=2$ spin system under the influence of a general anisotropic ZFS Hamiltonian $\mathscr{H}_{\rm ZFS}$. Energy is plotted as a function of the E/D ratio. Labels denote the eigenstates ($\pm2,\pm1,0$) of $\mathscr{H}_{\rm ZFS}^{(D)}$ at $E/D=0$.

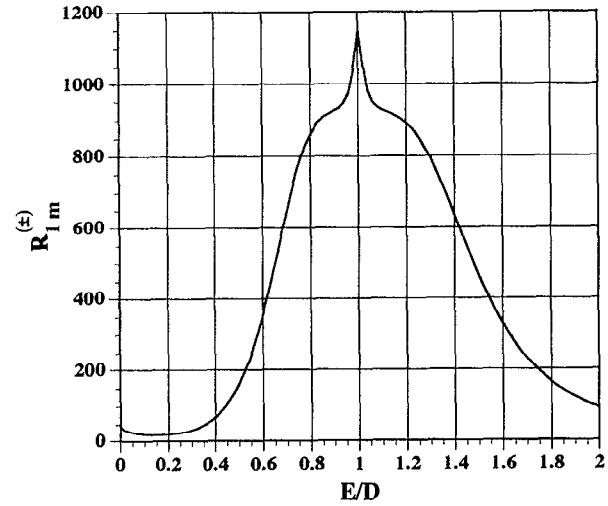

FIG. 8. Dependence of $\hat{R}_{1m}^{(\pm)}$ [defined by Eq. (6b)] on the ratio of ZFS parameters E/D in the ZFS limit.

which involves a much more abrupt crossing of $|\mu_2\rangle$ and $|\mu_4\rangle$. The effect of these level crossings on the behavior of $\hat{R}_{1m}^{(\pm)}$ is shown in Fig. 8. The calculations in the figure were carried out using the anisotropic ZFS-limit theory of Ref. 9. When $E/D\approx1$, R_{1m} exhibits resonant behavior which originates in the $\hat{R}_{1m}^{(\pm)}$ term. The resonance has broad and narrow components, both centered at $E/D=1$, which correspond to the two level crossings in Fig. 7. The ratio of amplitudes of the broad and narrow components of $\hat{R}_{1m}^{(\pm)}$ is 0.8:0.2.

VI. ANGULAR DEPENDENCE OF THE NMR PRE

Both the resonant and nonresonant parts of R_{1m} are functions of Θ and Φ, the polar angles which specify the position of the nuclear spin in the molecular coordinate system.[9] The functional dependence on Θ is shown in Fig. 9, where curves are plotted for three Θ values, $\Theta=0$, $\Theta=0.9553$, and $\Theta=\pi/2$. The curves for $\Theta=0$ and $\Theta=\pi/2$ correspond to extremes in the angular variation of R_{1m}. The angle $\Theta=\Theta_0$ with $\Theta_0\equiv0.9553$ rad is the polar angle at which the second degree Legendre polynomial $P_2(\cos\Theta)$ equals zero. This curve corresponds to values of R_{1m} that are averaged over the space of Θ (see below).

It should be noted in Fig. 9 that the resonant and nonresonant parts of R_{1m} have opposite Θ dependence. The nonresonant term $\hat{R}_{1m}^{(z)}$ exerts a greater influence on axial nuclear positions than on equatorial nuclear positions; the opposite Θ dependence occurs for the resonant term $\hat{R}_{1m}^{(\pm)}$. This difference reflects differing geometries of the local magnetic dipole fields that are associated with the resonant and nonresonant parts of R_{1m}.[9] The functional form of the Θ dependence is the same as that which occurs in the uniaxial ZFS-limit theory, namely,

$$\hat{R}_{1m}^{(z)} \propto 1+P_2(\cos\Theta),$$

$$\hat{R}_{1m}^{(\pm)} \propto 1-2^{-1}P_2(\cos\Theta).$$

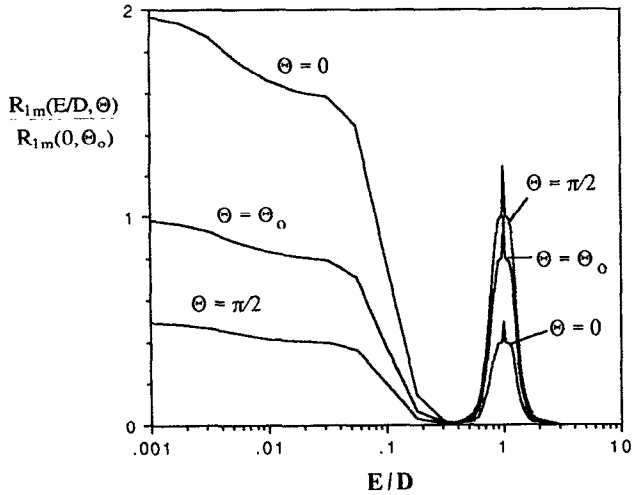

FIG. 9. Angular dependence of the NMR PRE in the anisotropic ZFS limit as a function of the ratio of the ZFS parameters E/D for three values of the polar angle Θ. The calculations are normalized to the value of R_{1m} at $E/D=0$, $\Theta=\Theta_0=0.9553$ rad.

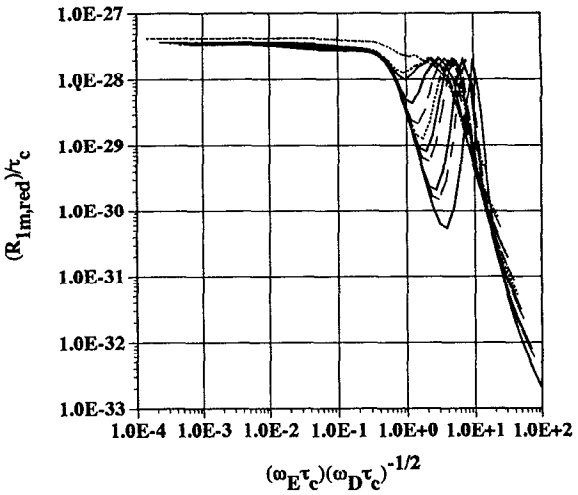

FIG. 10. Proposed parametrization of NMR-PRE data for $S=2$ in the anisotropic ZFS limit. Twelve calculated curves of $(R_{1m,\mathrm{red}}/\tau_c)$ vs $\chi\equiv(\omega_E\tau_c)(\omega_D\tau_c)^{-1/2}$ are shown corresponding to the combinations of three values of the ZFS parameter D and four values of the dipolar correlation time τ_c. Solid lines are for $D=5$ cm^{-1}, dashed lines are for $D=3$ cm^{-1}, and dotted lines are for $D=1$ cm^{-1}. The four solid lines correspond to four values of τ_c, $\tau_c=10$, 25, 50, and 100 ps, the longest τ_c value having the deepest local minimum in the region $\chi=1$–4. The families of four dashed lines and four dotted lines are similarly ordered in that the deepest minimum corresponds to the longest τ_c value.

Since $\overline{P_2(\cos\Theta)} = P_2(\cos\Theta_0) = 0$, the curve for Θ_0 in Fig. 9 corresponds to an average of R_{1m} over the space of Θ as pointed out above.

In addition to Θ dependence, the resonant term exhibits Φ dependence when $\mathscr{H}_{\mathrm{ZFS}}$ is anisotropic. As shown previously,[9] $\hat{R}_{1m}^{(\pm)}$ can be written as a sum of terms, one of which is Θ dependent but Φ independent, the other of which transforms as $\hat{x}^2-\hat{y}^2$. The nonresonant term $\hat{R}_{1m}^{(z)}$ is strictly Φ independent. The calculations of Fig. 9 were carried out for $\Phi=\pi/4$, where all Φ dependence in $\hat{R}_{1m}^{(\pm)}$ vanishes.

VII. CRITERIA FOR NEGLECT OF RHOMBIC COMPONENTS IN THE ZFS TENSOR

In the vicinity of the ZFS limit, it is frequently the situation that NMR-PRE phenomena are largely independent of the specific numerical value of the ZFS parameter D. This occurs because ω_D appears only in $\hat{R}_{1m}^{(\pm)}$, not in $\hat{R}_{1m}^{(z)}$, and when $\omega_D\tau_c>1$, $\hat{R}_{1m}^{(\pm)}$ is small as long as $E/D\ll 1$. This approximate independence of the NMR PRE on ω_D is fortunate, since independent experimental information on the ZFS parameters is usually unavailable for the chemical systems used in NMR studies. While it is approximately independent of ω_D, $\hat{R}_{1m}^{(z)}$ is quite sensitive to the magnitude to the E/D ratio. In this section we discuss criteria for deciding when the effects of rhombicity in the ZFS tensor can appropriately be neglected, and more generally, the conditions under which NMR-PRE data can be analyzed quantitatively in the absence of experimental information on the ZFS parameters E and D.

From the above discussion, it is expected that ZFS anisotropy will be important when significant precession of $\hat{S}_z$ occurs over the coherence time scale that is defined by τ_c. For $S=2$, the precessional frequencies of $\hat{S}_z$ are the eigenfrequencies ω_1 and ω_4, with ω_1, which accounts for 80% of the magnitude of $G_z(0)$, much more important. Thus, the effect of ZFS anisotropy becomes important when $\omega_1\tau_c>1$ and when $\omega_4\tau_c>1$ for the large and small terms, respectively. In order to obtain a parametrization in terms of the ZFS parameters D and E, we have carried out numerous calculations of R_{1m} as a function of τ_c and of the ZFS parameters ω_D and ω_E, searching for the most efficient representation of the data. In these studies, R_{1m} was expressed in a reduced form, $R_{1m,\mathrm{red}}\equiv(\gamma_I g\beta r^{-3}\mu_0/4\pi)^{-2}R_{1m}$, to suppress simple scaling factors. Optimal results were obtained for plots of $(R_{1m,\mathrm{red}}/\tau_c)$ vs the dimensionless parameter $\chi\equiv(\omega_E\tau_c)(\omega_D\tau_c)^{-1/2}$, as shown in Fig. 10. For a wide range of D, E, and τ_c, the large (80%) drop in $\hat{R}_{1m}^{(z)}$ begins when $\chi\gtrsim 0.4$. The same parameter χ does not as effectively parametrize the resonant part of R_{1m}, which is centered about $E/D=1$, nor the small (20%) component of $\hat{R}_{1m}^{(z)}$ that is due to ω_4. Clearly the depth and breadth of the R_{1m} minimum varies within the range $\chi=0.5$–10. However, the χ parametrization does provide a useful basis for deciding when the effects of ZFS anisotropy can appropriately be ignored. The appearance of the factor $\omega_E\tau_c$ in the parameter χ is not surprising in view of its physical association with the precessional behavior of $\hat{S}_z$. Lacking an analytical theory for the anisotropic ZFS limit, however, we cannot at present give a full theoretical justification for the functional form of χ. It should also be noted that the criterion $\chi\lesssim 0.4$ is appropriate for $S=2$, but probably not for other spin values, for which different criteria and perhaps also different parametrizations may be needed.

The parametrization shown in Fig. 10 is very effective for the major part of $\hat{R}_{1m}^{(z)}$ for the $S=2$ spin system. More generally, it also specifies the range of experimental conditions under which ZFS-limit NMR-PRE data can be ana-

lyzed quantitatively without specific experimental information concerning the magnitude of the ZFS interaction. Specifically, the condition $\chi \lesssim 0.4$ specifies the experimental ZFS-limit regime in which R_{1m} is largely independent of both of the ZFS parameters D and E. In this regime, the expression

$$R_{1m} \cong b_z(r,\Theta)\left(\frac{S(S+1)}{3}\right) j(\omega_I)$$

is reasonably accurate.

VIII. INTERPRETATION OF NMR-PRE DATA FOR Mn[acac]$_3$

tris-[acetylacetonato]Mn(III) (Mn[acac]$_3$) is a model $S=2$ complex, the spin relaxation properties of which have been studied previously in considerable detail.[5,6,8,24,25] This complex contains high-spin Mn(III), a d^4 ion that is subject to Jahn–Teller distortion. This results in tetragonal elongation of the oxygen coordination sphere, which, in Mn[acac]$_3$, has approximate D_{4h} symmetry, with four short Mn–O bonds [1.942, 1.931, 1.934, and 1.933 Å, r_{av}(Mn–O) = 1.935 Å] and two long Mn–O bonds [2.112 and 2.109 Å, r_{av}(Mn–O) = 2.111 Å].[26] The ZFS of Mn[acac]$_3$ is substantial [$D = -3.1$ cm^{-1} (Ref. 27)] and, judging from the near tetragonal symmetry of the manganese coordination sphere, approximately uniaxial. Previous theoretical analyses of the methyl proton resonances of Mn[acac]$_3$ are described in Refs. 6 and 25. These analyses included the effects of the uniaxial ZFS and Zeeman interactions but ignored the effects of ZFS rhombicity. In this section we examine the role of ZFS rhombicity on the analysis and in particular on the uncertainties that are associated with our lack of knowledge of the magnitude of the ZFS parameter E.

To examine this question, we have calculated the dependence of R_{1m} for the methyl proton resonance on the E/D ratio, employing in the calculations the same parameters, $|D| = 3.1$ cm^{-1}, $\tau_S = 8$ ps, $\Theta = 0.95$, that were used in the study of Ref. 6. Using these values of τ_S and $|D|$, the criterion suggested above ($\chi < 0.4$) implies that the uniaxial ZFS limit theory should be reasonably accurate for E/D ratios up to about 0.15 or $E < 0.5$ cm^{-1}. A detailed description of the dependence of R_{1m} on E/D is shown in Fig. 11, which was calculated assuming $\tau_S = 8$ ps and $|D| = 3.1$ cm^{-1}. This curve is qualitatively similar to that of Fig. 9, but exhibits quantitative differences due to the relatively small value of the reduced dipolar correlation time ($\omega_D \tau_c = 1.6$). The high frequency feature due to ω_4 is shifted to higher E/D values, the midpoint now occurring in the vicinity of $E/D = 0.04$. Also, the resonant features near $E/D = 1$ are broadened, and the depression in R_{1m} which occurs near $E/D = 0.35$ is much less pronounced.

From Fig. 11 it is clear that the ZFS rhombicity acts to depress R_{1m} below the value that would occur if the ZFS tensor were uniaxial ($E/D = 0$). The effect of this in the analysis is that the calculated dipolar correlation time τ_c (which for Mn[acac]$_3$ is nearly equal to τ_S) computed from uniaxial ZFS-limit theory is smaller than the true

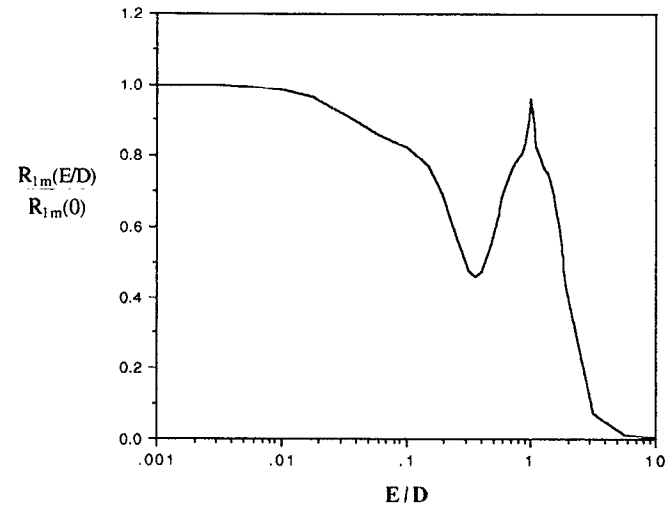

FIG. 11. Effect of ZFS anisotropy on the NMR PRE of *tris*-(acetylacetonato)Mn(III) in the anisotropic ZFS limit. The calculations assumed $|D| = 3.1$ cm^{-1} and $\tau_S = 8$ ps, and are normalized to the value of R_{1m} at $E/D = 0$.

value. Figure 11 provides a basis for estimating this error as a function of the E/D ratio. When E/D is very small ($E/D < 0.02$), the attendant error in τ_S is negligible, 0%–2%. For moderate E/D values, $0.02 < E/D < 0.15$, R_{1m} undergoes its initial drop of 20%. The value of τ_S that is calculated by uniaxial ZFS-limit theory is thus smaller than the true value by a factor that increases from 2% to 20% across this range. For $E/D > 0.15$, the error increases more rapidly. The maximum possible error in τ_S due to ZFS rhombicity is approximately a factor of 2, which occurs at the R_{1m} minimum at $E/D = 0.4$.

The ZFS parameter E of Mn[acac]$_3$ has not been measured; however, the degree of chemical anisotropy in the transverse plane of Mn[acac]$_3$ is not large. The E/D ratio can be estimated crudely by considering as a ratio the variation of Mn–O bond lengths within the transverse plane relative to the difference between the axial and equatorial Mn–O bond lengths. This comparison suggests that E/D is the order of 0.05. On this basis it is likely that τ_S was underestimated slightly, by 10%–20%, in previous studies, in other words, that $\tau_S = 9$–10 ps rather than 8 ps.

This is a very minor difference. However, it is clear from Fig. 9 that in general the effect of the E term of the ZFS tensor can become quite large when $\chi > 0.4$, particularly when $\omega_D \tau_c \gg 1$. In practical cases, the likely influence of ZFS rhombicity on the NMR PRE needs careful consideration in experimental studies that are conducted outside the Zeeman limit.

APPENDIX

Matrix representations of the first- and second-rank spherical tensor operators for $S = 2$ are given below:

$$S_0^{(1)}=S_z=\begin{pmatrix}2&0&0&0&0\\0&1&0&0&0\\0&0&0&0&0\\0&0&0&-1&0\\0&0&0&0&-2\end{pmatrix},$$

$$S_{+1}^{(1)}=-2^{-1/2}S_+=-2^{-1/2}\begin{pmatrix}0&2&0&0&0\\0&0&6^{1/2}&0&0\\0&0&0&6^{1/2}&0\\0&0&0&0&2\\0&0&0&0&0\end{pmatrix},$$

$$S_{-1}^{(1)}=2^{-1/2}S_-=2^{-1/2}\begin{pmatrix}0&0&0&0&0\\2&0&0&0&0\\0&6^{1/2}&0&0&0\\0&0&6^{1/2}&0&0\\0&0&0&2&0\end{pmatrix}.$$

Matrix representations of the second-rank spherical tensor operators which appear in Eq. (2c) are

$$\hat{S}_0^{(2)}=\left(\frac{3}{2}\right)^{1/2}\begin{pmatrix}2&0&0&0&0\\0&-1&0&0&0\\0&0&-2&0&0\\0&0&0&-1&0\\0&0&0&0&2\end{pmatrix},$$

$$\hat{S}_{+2}^{(2)}+\hat{S}_{-2}^{(2)}=\begin{pmatrix}0&0&6^{1/2}&0&0\\0&0&0&3&0\\6^{1/2}&0&0&0&6^{1/2}\\0&3&0&0&0\\0&0&6^{1/2}&0&0\end{pmatrix}.$$

The forms of these operators follow from the relations $S_0^{(2)}=6^{-1/2}[3(S_z)^2-S(S+1)]$ and $S_{\pm 2}^{(2)}=2^{-1}(S_\pm)^2$.[28]

[1] I. Solomon, Phys. Rev. **99**, 559 (1955).
[2] N. Bloembergen, J. Chem. Phys. **27**, 572 (1957); **27**, 595 (1957).
[3] N. Bloembergen and L. O. Morgan, J. Chem. Phys. **34**, 842 (1961).
[4] R. R. Sharp J. Chem. Phys. **93**, 6921 (1990).
[5] T. Bayburt and R. R. Sharp, J. Chem. Phys. **92**, 5892 (1990).
[6] R. R. Sharp, J. Magn. Resonance **100**, 491 (1992).
[7] R. R. Sharp, J. Chem. Phys. **98**, 912 (1993).
[8] R. R. Sharp, J. Chem. Phys. **98**, 2507 (1993).
[9] R. R. Sharp, J. Chem. Phys. **98**, 6092 (1993).
[10] U. Lindner, Ann. Phys. (Leipzig) **16**, 319 (1965).
[11] D. T. Pegg, D. M. Doddrell, M. Robin Bendall, and A. K. Gregson, Aust. J. Chem. **29**, 1885 (1976).
[12] D. T. Pegg and D. M. Doddrell, Aust. J. Chem. **31**, 475 (1978).
[13] H. L. Friedman, M. Holz, and H. G. Hertz, J. Chem. Phys. **70**, 3369 (1979).
[14] T. R. Chen, S.-J. Den, and L.-P. Hwang, Proc. Natl. Sci. Counc. (Rep. China) A **8**, 224 (1984).
[15] L.-P. Hwang and C.-Y. Ju, J. Chem. Phys. **83**, 3775 (1985).
[16] P.-L. Wang, J.-H. Lee, S.-M. Huang, and L.-P. Hwang, J. Magn. Reson. **73**, 277 (1987).
[17] N. Benetis, J. Kowaleski, L. Nordenskiold, H. Wennerstrom, and P.-O. Westlund, Mol. Phys. **48**, 329 (1983).
[18] N. Benetis, J. Kowalewski, L. Nordenskiold, H. Wennerstrom, and P.-O. Westlund, Mol. Phys. **50**, 515 (1983).
[19] P.-O. Westlund, H. Wennerstrom, L. Nordenskiold, J. Kowalewski, and N. Benetis, J. Magn. Reson. **59**, 91 (1984).
[20] N. Benetis and J. Kowaleski, J. Magn. Reson. **65**, 13 (1985).
[21] L. Banci, I. Bertini, F. Briganti, and C. Luchinat, J. Magn. Reson. **66**, 58 (1986).
[22] S. Szymanski, A. M. Gryff-Keller, and G. Binsch, J. Magn. Reson. **68**, 399 (1986).
[23] H. Fukui, K. Miura, and H. Matsuda, J. Magn. Reson. **88**, 311 (1990).
[24] D. T. Pegg, D. M. Doddrell, M. R. Bendall, and A. K. Gregson, Aust. J. Chem. **29**, 1885 (1976).
[25] T. Bayburt and R. R. Sharp, J. Phys. Chem. (in press).
[26] B. R. Stults, R. S. Marianelli, and V. W. Day, Inorg. Chem. **18**, 1853 (1959).
[27] A. K. Gregson, D. M. Doddrell, and P. Healy, Inorg. Chem. **17**, 1216 (1978).
[28] H. A. Buckmaster, R. Chatterjee, and Y. H. Shing, Phys. Status Solidi A **13**, 9 (1972).